Fire and vegetation dynamics in North-West Siberia during the last 60 years based on high-resolution remote sensing

Oleg Sizov[1,*], Ekaterina Ezhova[2,*], Petr Tsymbarovich[3], Andrey Soromotin[4], Nikolay Prihod'ko[4], Tuukka Petäjä[2,4], Sergej Zilitinkevich[2,5], Markku Kulmala[2,4], Jaana Bäck[6], and Kajar Köster[6]

[1]Institute of Oil and Gas Problems Russian Academy of Science, Moscow, Russia
[2]Institute for Atmospheric and Earth System Research (INAR)/Physics, University of Helsinki, Finland
[3]Institute of Geography Russian Academy of Science, Moscow, Russia
[4]Tyumen' State University, Tyumen', Russia
[5]Finnish Meteorological Institute, Helsinki, Finland
[6]Institute for Atmospheric and Earth System Research (INAR)/Forest Sciences, University of Helsinki, Finland
[*]These authors contributed equally to this work.

Correspondence: Ekaterina Ezhova (ekaterina.ezhova@helsinki.fi)

Abstract. Rapidly warming Arctic undergoes transitions that can influence global carbon balance. One of the key processes is the shift towards vegetation types with higher biomass underlining a stronger carbon sink. The shift is predicted by the bioclimatic models based on abiotic climatic factors but it is not always confirmed with observations. Recent studies highlight the role of disturbances for the shift. Here we use high-resolution remote sensing to study the process of transition from tundra to forest and its connection to wildfires on the 20 000 km^2 area in North-West Siberia. Overall, 40% of the study area was burned during 60-yr period. Three quarters of the burned areas were dry tundra. About 10% of the study area experienced 2-3 fires with an interval of 15-60 years suggesting a shorter fire return interval than that reported earlier for the northern areas of Central Siberia (130-350 years). Based on our results, the shift in vegetation (within the 60-years period) occurred in 40-85% of the burned territories. All fire-affected territories were flat, therefore no effect of topography was detected. Oppositely, in the undisturbed areas, transition of vegetation was observed only in 6-15% of the territories, characterized by steeper topographic slopes. Our results suggest a strong role of disturbances for the tree advance in North-West Siberia.

1 Introduction

North-West Siberia is the region subject to a strong warming trend in summer as compared to the Arctic average. The annual warming trend reported for the entire Arctic (1971-2017) is 0.6°C per decade, resulting from the cold season trend of 0.7°C per decade, and the warm season (June-September) trend of 0.4°C per decade (Box et al., 2019). According to the 2nd Assessment report on the climate change on the Russian territory (Katsov et al., 2014), the winter warming trend in North-West Siberia (1972–2012) is 0.4-0.7°C per decade, which is comparable to the trends reported for the entire Arctic. However, the summer trend is 0.8-1.0°C per decade, double that is reported for the entire Arctic. At the same time, meteorological observations indicate that snow cover thickness increased at the rate 2-10 cm per decade but the number of snow cover days decreased at the rate up to 8 days per decade (Katsov et al., 2014). An increase in warm degree-days favors a shift of vegetation type towards more southern species, i.e., transformation of tundra environment into shrubs and forest vegetation. Shrubs and trees decrease surface albedo and have a warming effect, especially in winter, but the higher amount of biomass will increase the terrestrial carbon sink. Forest ecosystems can additionally enhance carbon uptake via complex atmosphere-biosphere feedback mechanisms (Kulmala et al., 2013; Kalliokoski et al., 2019; Kulmala et al., 2020).

Shrubification of tundra has been reported in many recent studies (Myers-Smith and Hik, 2018; Maliniemi et al., 2018; Bjorkman et al., 2020) and it has been associated with Arctic greening (Myers-Smith et al., 2020). However, there is no general agreement regarding tree propagation. Modelling studies predict tree-line advance to the north based on abiotic factors (Tchebakova et al., 2010; Kaplan and New, 2006; Aakala et al., 2014). Nevertheless, this advance has been only partially confirmed by observations (Harsch and Bader, 2011) and the observed rates are extremely low as compared to the theoretical predictions (Van Bogaert et al., 2011). On the contrary, the study based on the forest inventories from the eastern United States shows that forested areas shrink rather than expand on most plots at their range limits (Zhu et al., 2012). These discrepancies suggest that there exist other factors than climatic ones influencing the transition. First, Frost and Epstein (2014) found it to be dependent on another abiotic factor: a topographic slope. Different topographic slopes result in different insolation, moisture regime and permafrost state. Second, it was hypothesized that biotic factors interact with abiotic climatic factors (Woodward et al., 2004). Availability of seeds, germination success and presence of dominant species competing with newly establishing plants can all influence propagation of the tree-line. A recent study suggests that the shift of biomes occurs episodically and requires a disturbance (Renwick and Rocca, 2015). In northern latitudes (boreal, subarctic and arctic areas), wildfires and grazing by reindeer are the two main disturbances that influence the vegetation structure and dynamics (Köster et al., 2013; Narita et al., 2015), which in turn induce shifts in ecosystem processes, e.g. nutrient cycles and ecological interactions.

The reindeer regulate the abundance of species and community composition via grazing. Both observations and field experiments in tundra show different response to warming with and without large herbivores (Post and Pedersen, 2008; Olofsson et al., 2009), manifested by an enhanced growth of deciduous shrubs on sites not affected by grazing. However, evergreen shrubs and trees demonstrate an opposite trend towards an increased growth on sites exposed to grazing (Bernes et al., 2015). The effect of wildfires on the vegetation shift in tundra is less studied. Fire has been found to reduce the cover of lichens and bryophytes (Joly et al., 2009), but enhance the growth of grasses and shrubs (Barrett et al., 2012; Narita et al., 2015). Landhausser and Wein (1993) observed that forests in the Canada's Northwest Territories advance in the forest-tundra ecotone after a strong wildfire. Long before that, Sannikov et al. (1970) noted that seedlings' survival is highest on bare mineral soils, and high intensity and severity wildfires, which remove the organic material and expose mineral soil, can favor tree survival.

Here we study the shift in vegetation based on high-resolution remote sensing data, in the areas including southern tundra, forest-tundra ecotone and northern taiga in the Nadym-Pur district of North-West Siberia. Opposite to northerly-located Yamal and Gydan peninsulas and westerly-located Priuralsky district, these areas have not yet suffered from reindeer pasture overuse (Matveev and Musaev, 2013). Therefore, grazing could be of secondary importance for the ecosystem changes in these areas. We hypothesize, based on the study of Landhausser and Wein (1993), that forest expansion occurs mainly in the areas affected by relatively recent wildfires, while other areas (non-disturbed areas) demonstrate only a minor change in vegetation. Thus, we focus on the effect of wildfires on the vegetation, specifically on tundra-forest and tundra-woodlands transition. The main objectives of this study are:

1) to assess the dynamics of regional climatic factors and the possibility of vegetation shifts due to climate change, in particular tundra-forest transition;

2) to quantify burned surface areas and calculate frequency of wildfires;

3) to study the link between wildfires and dry tundra transition to woodlands and forest.

Finally, we take into account physiographic characteristics of the landscape and study the link between the transition and the topographic slope.

2 Materials and methods

2.1 Field sites

In order to study tundra-forest transition, we selected the monitoring sites satisfying two predefined criteria:

1) the sites are covered by historical high-resolution satellite imagery - Corona archive (Ruffner, 1995);

2) the sites have forest cover less than 10% according to the Landsat forest mask (Hansen et al., 2013).

Based on these criteria, we identified three main study areas (Table 1, Fig. 1). Area 1 (the largest area) is located on the east coast of the river Nadym, area 2 is between the south coast of the Gulf of Ob' and river Yarudey and area 3 is to the west from the city of Nadym (Fig. 1). Detailed maps of the study sites can be found in geoportal 'Nadym. Changes in 50 years (1968-2018) (NC50)' (https://ageoportal.ipos-tmn.ru/nadym/). Description of the geoportal is given in Appendix A.

Northern part of study area 1 is in the continuous permafrost zone, while its southern part and study areas 2 and 3 are in the discontinuous permafrost zone (Trofimova and Balybina, 2015). The vegetation zones include southern tundra, forest-tundra ecotone and northern taiga (Ilyina et al., 1985), with the treeline crossing the study sites (Walker et al., 2005; MacDonald et al., 2008). Southern tundra zone is represented by dwarf-shrub, moss and lichen tundra, polygonal peatlands and dwarf-shrub, lichen woodlands. Vegetation community of the forest-tundra consists of larix and spruce-larix, dwarf-shrub moss woodlands and dwarf-shrub lichen tundra. Northern taiga is represented by larix and spruce-larix dwarf-shrub and moss-lichen forests and shrub-moss-lichen wetlands in flat or hilly terrain. The boundaries of these vegetation zones in the study areas, according to Ilyina et al. (1985), are shown in Fig. 1. Description of plant species and permafrost state at several sites obtained during the field campaign in 2019 is provided in Appendix B.

In addition, Fig. 1 shows the forest mask derived from the topographic maps by Ilyina et al. (1985). Forested areas include dense forests, shrubs in the floodplains and river deltas, forest sprouting. Overall, 3570 km^2 or 17.5% of the total study area was covered by forests, out of which 15.5% was dense forest, 1.2% - forest sprouting and less than 1% - shrubs. Dry tundra ('moss and lichen tundra' in the topographic maps) covered 11 370 km^2 or 55.7% of the total study area.

Anthropogenic activity in the study areas includes oil and gas mining (fields Medvezhye and Yarudeyskoe, major gas pipelines Yamburg-Tula, Yamburg-Yelets, SRTO-Ural, Urengoy-Center, Urengoy-Uzhgorod). The first geological surveys started in 1950s and the industrial exploration of the areas started in 1967. New railway road 'Northern Latitudinal Railway'

(Salekhard-Novy Urengoy) is currently under construction within study area 1. Environmental impact due to anthropogenic activities and climate change has been monitored since 1970s (Matyshak et al., 2017a, b; Sizov and Lobotrosova, 2016; Kukkonen et al., 2020).

2.2 Calculation of climatic indices

In order to assess the climatic conditions in the region, we used meteorological data (http://meteo.ru, latest access July 2019) from three stations, Novy Port, Nyda and Nadym (Supplementary material, SM), located along a 200-km latitudinal transect from the north (67.4N, Novy Port) to the south (65.3N, Novy Port). Station Novy Port (67°41'N, 72°52'E, 12 m a.s.l.) is located to the north of the study areas. This is the closest station to the northern boundaries of the study areas. Station Nyda (66°37'N, 72°57'E, 10 m a.s.l.) is located within study area 1. Station Nadym (65°32'N, 72°32'E, 7 m a.s.l.) is located near the southern borders of the study areas (50 km from study area 3). The data set contained 52 years of quality-checked meteorological observations (from 1966 to 2018), including air temperature (time resolution 3 h), precipitation (time resolution 12 h), and cloudiness 0 to 10 (time resolution 3 h). Based on this data set, we calculated the mean monthly temperatures (the sum of daily mean temperatures divided by the number of days in a month), monthly cumulative precipitation (the sum of daily precipitation measurements for a given month), the daily minimum and maximum temperatures for all the years and the mean annual temperature and annual precipitation.

In order to assess climatic factors influencing vegetation dynamics, we studied the length and mean temperature of the growing season, which we define as the period with daily mean temperatures above +5°C (Tchebakova et al., 1994). We calculated growing degree-days following Tchebakova et al. (1994),

$$GDD_5 = \sum_{\overline{T} \geq 5} (\overline{T} - 5), \tag{1}$$

where $\overline{T}$ - is the daily mean temperature [°C]. Another important abiotic factor for vegetation is humidity. We calculated potential evapotranspiration (PET) from the temperature and cloudiness measurements using Bonan's modification (Bonan, 1989) of Taylor-Priestley model (Priestley and Taylor, 1972). We used PET and precipitation to calculate a dryness index (DI) (Tchebakova et al., 1994), i.e. the ratio between annual PET and precipitation (P):

$$DI = \frac{PET}{P}. \tag{2}$$

Based on GDD_5 and DI, we classified the vegetation zones in Novy Port, Nyda and Nadym using the thresholds introduced in bioclimatic model SiBCliM (see Table 2 based on the data from Tchebakova et al. (1994)). Due to the fact that the stations are located along the latitudinal transect close to the study sites, they should be representative of their vegetation state.

2.3 Wildfires

The initial state of the study areas was assessed using Corona imagery. Corona is the US program from 1958 – 1972, which used satellite surveillance systems to get high-resolution photographic coverage from USSR-China and some other territories

(Ruffner, 1995). The ground resolution of the imagery for subsequent KH-1 to KH-4 missions continuously improved from 12 m (KH-1, 1960) to 2 m (KH-4, 1967). We identified 21 frames under clear-sky conditions from 21 August 1968. Each frame consisted of 4 scanned fragments. The cropped fragments without color correction were georeferenced to the chosen orthomosaic (SPOT layer, sec. 2.4) using 3rd degree polynomial method in software ArcGIS (v. 10.4.1). The r.m.s. error of georegistration estimated using control points did not exceed 10-12 m. Then the fragments were organized in separate paths and finally a mosaic was formed using mosaic operator Last in ArcGIS. This mosaic characterized the state of study areas at the start of the active industrial exploration of the region (1967).

Further, we used Landsat Level 1 data to quantify burned areas for particular years within 1968-2018 (Wulder et al., 2019). The data providing the best coverage of the study areas were available from the following years: 1988, 2001, 2016 and 2018 (Table 3). The images were synthesized using near- and mid-infrared channels (Landsat 5 and 7: 0.63-0.69 μm, 0.76-0.90 μm and 1.55-1.75 μm; Landsat 8: 0.64-0.67 μm, 0.85-0.88 μm and 1.57-1.65 μm) as burned areas are identifiable in the infrared range of wavelengths. Landsat mosaics for all years were formed after color correction using mosaic operator Blend in ArcGIS.

Mapping and quantification of the burned areas were performed by means of an object-based image analysis, successfully used for studies of landscape dynamics (Blaschke, 2010). On the first stage, we performed segmentation of mosaics using algorithm 'Multiresolution segmentation' in software eCognition (v. 9.0). The segmentation was done using parameters 40 for Scale and 0.5 for Color. The second stage, classification, was different for Corona and Landsat mosaics. In Corona mosaics, the spectral information was missing and we had to rely on the contrast of colors between non-disturbed tundra and burned areas. For visual classification we applied two criteria. First, non-disturbed tundra is lighter due to the presence of lichen in vegetation community, whereas recently burned areas are dark. Second, burned areas are characterized by well-defined boundaries often coinciding with river coastlines. An example illustrating segmentation and the visual choice of burned areas is shown in Fig 2. For Landsat mosaics, we used unsupervised classification ISODATA (15 classes, a change threshold 5%). Further, we identified visually one or two classes corresponding to burned areas. The segments containing more than 90% of pixels within these classes were identified as burned areas. The segments with 40-90% of pixels within these classes, located at the perifery of large fires, were added to burned area based on visual imagery check. Calculation of the areas of segments classified as burned areas was performed using standard instrument Calculate geometry in ArcGIS.

We studied the percentage and distribution of the burned sites and calculated the frequency of fire return. Corona and Landsat images showed that some years were characterized by particularly large-scale fires in the study areas (see an example for 1990 in SM, Fig. SB1). These years are referred to as the years of major fires. The burned areas can be detected in the satellite images during a few years after the fire. Burned areas in Corona mosaic from 1968 were partially dated back to the fires in the period 1953-1964 based on geological surveys and early Corona images (the sources are listed below Table 4). Landsat mosaics from 1988, 2001, 2016 and 2018 largely reflect the state of the study areas after the major fire years 1976, 1990, 2012 and 2016 (Table 4). For a given territory, the fire interval was calculated as the difference in years between the major fires.

2.4 Vegetation dynamics

We have studied the vegetation dynamics using two methods. First, we used Normalized Difference Vegetation Index (NDVI) distributions to assess the state of vegetation in the sites burned at different times. Second, we studied the tundra-forest shift of dry tundra during the period of ca 60 years visually comparing historical imagery to modern satellite data of high spatial resolution. A similar visual method was used by e.g. Frost and Epstein (2014) to study transition from grassland to shrubs in northern Eurasia.

Below we describe the method based on NDVI. This index reflects the state of biomass, i.e. vegetation greenness, density and development (Walker et al., 2003; Johansen and Tømmervik, 2014; Miles and Esau, 2016). NDVI was calculated from the visible (VIS) and near-infrared (NIR) radiation reflected by vegetation:

$$NDVI = \frac{NIR - VIS}{NIR + VIS}. \tag{3}$$

We chose two scenes from one path of Landsat-8 from 30 June 2018 (Table 5). We used Level 2 data (CEOS) after atmospheric correction by the standard Landsat 8 OLI atmospheric correction algorithm (Vermote et al., 2016). NDVI was calculated in ArcGIS using standard tools.

We analysed NDVI distributions for study area 1, separately for dry tundra burned in different years (as detected in satellite imagery mosaics from 1968, 1988, 2001, 2018) and for non-disturbed dry tundra. We considered the territories covered by one satellite overpass. Moreover, analysis of burned tundra included only the sites burned once within 60 years. In order to make the study areas more balanced by size, we merged the data sets from the burned territories detected in 1968 and 1988, for which we might expect that vegetation had recovered after the fires, and omitted 2016 due to insufficient size of the fire-affected territory. As a result, all study areas were larger than 600 km^2 (1968+1988 – 600 (405+195) km^2, 2001 – 1565 km^2, 2018 – 867 km^2, non-disturbed – 937 km^2). Using the dates of major fires (Table 4) and the date of Landsat mosaic (2018), we can assume that NDVI within burned tundra sites detected in 1968 and 1988 reflect the state of vegetation after fires more than 42 years ago, in 2001 – after fires 28 years ago, in 2018 – after fires 2 years ago. NDVI in non-disturbed tundra refers to tundra not affected by fires during the whole study period.

The visual method can be described as follows. The data sets used in the analysis of vegetation dynamics are summarized in Table 5. The initial state of vegetation was assessed using Corona mosaic (Section 2.3) and topographic maps. The topographic maps were used to develop forest and dry tundra masks using automatic tracing in software EasyTrace (v. 8.7). The resulting vector layer was checked and corrected using Corona mosaic.

Assessment of the current state of vegetation was based on SPOT and Resurs-P data (Table 5). The study areas were almost fully covered by the mosaic of SPOT-6,7 imagery. Ca 10% of the study areas were covered by three paths of Resurs-P (product level 1C, channels B, G, R and NIR). Resurs-P data was co-registered to the SPOT mosaic in ArcGIS. The data were synthesized in the visible radiation range without color adjustment. The SPOT mosaic was used as a pluggable webmap layer without additional processing.

Firstly, based on the topographic map and Corona mosaic, we identified two types of dry tundra sites: those burned before 1968 (Sec. 2.3) and those not affected by fires during the whole study period. The area of burned tundra was 1090 km^2 and the area of non-disturbed tundra was 5300 km^2. Then we introduced random sample circles with 100 m diameter within the subsets. The samples were spaced at intervals of 2 km within burned tundra (157 samples) and at intervals of 5 km within non-disturbed tundra (231 sample). We included only the circles, for which we could confidently state that there were no trees in 1968. In the modern imagery, we distinguished between the following types of vegetation: tundra (no trees), woodland (trees covered less than 50% of the area inside the circle) and forest (trees covered more than 50% of the area inside the circle). We visually compared the areas inside the circles in the historical and modern images (see examples in Fig. 3). We introduced three change classes: 'no change', when tundra was identified both in the old and modern images, 'to woodlands', when tundra turned to woodlands and 'to forest' when tundra turned to forest.

2.5 Topographic slopes

To quantify the topographic slopes, we used a digital elevation model ArcticDEM (Table 5). The model is a mosaic with high spatial resolution (2 m). The stereo-couples for this version of the model were prepared in 2010-2017. It is currently the most detailed source of information on the relief. Co-registration of the mosaic elements, calculation of slopes and preparation of the raster layer for the geoportal NC50 (Appendix A) was done in ArcGIS.

We calculated topographic slopes within the circles where we visually assessed the vegetation shift. For calculation, we used the circles with 50 m diameter located in the centers of larger sample circles (Sec. 2.4). For each circle, we calculated the mean slope. We separated data corresponding to burned tundra and non-disturbed tundra and further stratified it by vegetation shift ('no shift', 'to woodlands', 'to forest'), thus splitting the data set into 6 classes. Finally, we calculated the median values, 25th and 75th percentiles of mean slopes for each class.

3 Results

3.1 Temperature, precipitation and climatic indices

During the last 50 years, the mean annual temperature at the meteorological stations has increased by 2.6-3.0°C (Fig. 4): from -9.5°C to -6.5°C in the north and from -6.5°C to -4°C in the south. In addition, the daily minimum temperature has increased by 4-5°C (from -44...-45°C to -40°C, SM, Fig. SA1-SA3).

The growing season typically lasts 3 months in the north and 3-4 months in the south (SM, Fig. SA1-SA4). The length of the growing season has increased by 24 days (SM, Fig. SA1-SA3): from 72 to 97 days in the north (Novy Port) and from 97 to 121 days in the south (Nadym). The mean temperature has increased by 1.0-1.4°C. In general, both the length and the mean temperature of growing season exhibit great variability particularly during recent years (SM, Fig. SA1-SA3). Following the mean temperature and the length of growing season, the growing degree-days, GDD_5, have increased over the last 50 years (Fig. 4). The strongest increase in GDD_5 (ca 200°C days) was observed during 20 years from 1966 to 1985, after which GDD_5 levelled off. The period from 1980 to 1995 seemed to be the most favorable period for a new forest establishment due to the relative stability of mean temperature and GDD_5. On the contrary, the last decade was characterized by a strong variability in both mean annual temperature (the peak-to-peak value was ca 3°C) and GDD_5 (the peak-to-peak value was larger than 400°C days), which could make seedlings' survival less probable.

Mean annual precipitation increases from the north to the south: from 330-340 mm in Novy Port to 510 mm in Nadym (SM, Fig. SA4). Precipitation in the northern part (Fig. 5) is characteristic of the arctic regime with the annual value below 400 mm, whereas precipitation in the southern part (Fig. 5) is characteristic of the temperate continental regime (Chorley, 1971). Monthly variability of precipitation follows a well-pronounced seasonal cycle (SM, Fig. SA4) with a maximum in August (July-August in the south). While the seasonal cycle of precipitation was similar in three stations, the inter-annual variability was not. Precipitation time series in Nyda and Novy Port were closely following each other between 1965 and 2005 (Fig. 5). Since 2005, the annual precipitation has drastically decreased in Novy Port and it has increased in Nyda. Potential evapotranspiration increased at all three sites. Accordingly, the dryness index (DI) increased from 0.4 to 0.5-0.6 everywhere (SM, Fig. SA5). During a few recent years, DI in Novy Port exceeded unity several times.

Based on the observed growing degree-days and DI, we assessed the change in the vegetation class at three stations (Table 6). The vegetation class has changed at two sites (Nadym and Novy Port). This is a result of an increase in GDD_5, while DI was not a limiting factor for the vegetation class at any of the three stations. Due to the fact that GDD_5 is a function of air temperature and the latter depends mainly on latitude, GDD_5 from the three stations should be representative of our study areas. Therefore, we can conclude that1) our study sites should have experienced vegetation change during 60 years, specifically from tundra to forest in the north; and 2) temperature and moisture regimes throughout our study areas are theoretically suitable for forests.

3.2 Dynamics of fires

Weather conditions in Northern Siberia can support large-scale wildfires during summer time. The fires occur mainly in July (Ponomarev et al., 2016). Burned areas after five major fire events (Table 4) are shown in Fig. 6a. The burned areas in Fig. 6a can overlap if the same site experienced more than one fire. Separate maps of the burned sites for each of five cases (Table 4) are available in geoportal NC50 (Appendix A).

The overall area of burned sites was ca 8300 km^2 constituting more than 40% of the total study area. Fig. 6b shows the distribution of the fraction of burned area over years. The largest fires, contributing more than 30% to the total burned area, occurred between 1989 and 2001 (mainly in 1990, Fig. SB1). The fires in each of the periods 1953-1968, 1968-1988 and 2016-2018 contributed 10-20% of the total burned area (Fig. 6b). In addition, ca 10% of that area was recognized both in 1988 and 2001 imagery. According to Fig. 6b, ca 80% of the burned area experienced fire once and 20% experienced fires more than once during 60 years. Approximately 17% of the fire-affected territory (1400 km^2) burned twice, 2.5% of the territory (200 km^2) burned three times and 0.2% (20 km^2) burned four times. These sites were characterized by a remarkably small period between consequent fires, which was estimated as 15-60 years if only major fires were taken into account (Table 4).

3.3 Vegetation dynamics and its link to fires and topography

3.3.1 Assessment of vegetation recovery after fire using Normalized Difference Vegetation Index (NDVI)

Fig. 7a shows study area 1 where we marked dry tundra burned in different time periods and non-disturbed dry tundra. Fig. 7b shows the corresponding distributions of NDVI. As discussed in Methods (Sec. 2.4), 1968+1988 data reflect the state of vegetation in the site burned more than 42 years ago, 2001 data – 28 years ago, 2018 data – 2 years ago and non-disturbed data refer to tundra not affected by fires during the whole study period.

In Fig. 7b, the NDVI distributions from the non-disturbed tundra and recently burned sites are close to Gaussian ones. Interestingly, the distributions from the sites burned 28 and >42 years ago are bimodal and they have higher NDVI values as compared to the non-disturbed and recently burned sites. We fitted the distributions by the sums of two Gaussian functions (the fits are shown in Fig. 7b) and determined mean values and standard deviations for all the peaks (Table S1). The positions of the lower peaks of the bimodal distributions differ only slightly, whereas the position of the upper peak is a bit lower and the peak is less pronounced for the distribution from the site burned 28 years ago.

Further, we used the mean values and standard deviations of the fitted Gaussian functions to identify vegetation associated with the peaks of the distributions. For illustration, we chose an image containing all representative examples of vegetation (Fig. 8). Green color in Fig. 8, right panel, indicates the sites with NDVI in the interval ($NDVI_{max,2}$-σ_2; $NDVI_{max,2}$+σ_2) corresponding to the upper peak of the distribution based on the data from 1968+1988. Comparing left panel and right panel of Fig. 8, one can conclude that this peak is mainly associated with forest. The lower peak (the areas in blue color in Fig. 8, right panel) corresponds to woodlands and tundra. This lower peak has a large intersection with the peak in the unimodal distribution from the non-disturbed site. However, interestingly, there is a significant decrease in the areas with NDVI below ca 0.52 in the bimodal distributions. These areas are marked in pink in Fig. 8, right panel. They correspond to the tundra sites lightest in color due to the presence of lichen in the vegetation community.

Finally, from the bimodal distributions we estimated the fraction of area occupied by forest. Using standard deviations of the two peaks, the boundary separating the forest peak from the tundra peak is NDVI = 0.72. We assumed that areas with NDVI > 0.72 represent mainly forest, and areas with NDVI < 0.72 – mainly tundra and woodlands. We integrated the bimodal distributions to find the fraction of area with NDVI > 0.72. Our estimates show that in the sites burned 28 years ago, forests occupy 19$\%$ of the total area. In the sites burned more than 42 years ago, the fraction of forest increased to 28$\%$ of the total area.

While precise calculations of the forest fraction based on NDVI are challenging, the main results following from Figs. 7, 8 can be summarized as follows:

1. The NDVI distributions based on the data from non-disturbed tundra and the sites burned 2 years ago are predominantly unimodal, whereas the distributions based on the data from the sites burned 28 years ago and earlier are bimodal.

2. The low-NDVI sites corresponding to vegetation communities in tundra with relatively high amounts of lichen and thus having the lightest colors in the images almost disappear from the distributions calculated for the vegetation communities recovered after fires.

3. Instead, the new state of vegetation recovered after fires is characterized by a higher mean NDVI due to the new peak associated with forest. The fraction of high-NDVI area representing forest increases with the time after the last fire.

3.3.2 Assessment of vegetation shift using visual method, connection to fires and topography

Fig. 9 illustrates the shift from dry tundra to other types of vegetation in the sites burned before 1968 (Fig. 6). The largest part of burned dry tundra was in the northern taiga zone, and relatively large part was in the forest-tundra ecotone. The burned area in southern tundra contained only 7 samples, therefore the corresponding results are not statistically reliable. The shift of vegetation indicated by green symbols is clearly seen in the forest-tundra, while it is less pronounced in the northern taiga.

Statistics of the vegetation shift is summarized in Table 7 and illustrated in Fig. 10. In the absence of disturbances, only a tiny fraction (ca 5%) of dry tundra turned to woodlands in the southern tundra zone, whereas a somewhat larger proportion (15%) of changing vegetation was observed in the forest-tundra and northern taiga (Table 7). Note that none of the non-disturbed dry tundra sites developed forest. On the contrary, burned dry tundra exhibited a significant shift towards tree-dominated vegetation: 85% of samples in the forest-tundra and 45% of samples in the northern taiga. More than 50% of samples showed change to forest in the forest-tundra ecotone (Table 7), and more than 10% of samples - in the northern taiga.

Finally, we assessed the link between the vegetation shift and topographic characteristics (Fig. 11). The shift was dependent on topography in the non-disturbed sites. The median value of the mean topographic slope was ca one degree in the areas with no detected shift, ca three degrees in the areas with the shift towards woodlands, and it increased to six degrees in the areas with the shift towards forest. Note that there were only five points in the non-disturbed areas with shift to forest, all of them were located in the river valleys (these points were not accounted in the statistics in Table 7). Oppositely, the slope dependence was weak or absent in the predominantly flat burned areas.

4 Discussion

Different climate models generally agree that the greatest warming due to the enhanced greenhouse gas emissions occurs at northern high latitudes (Sand et al., 2016). Studies show that the snowmelt and spring recovery occurs earlier in the Northern Hemisphere boreal and subarctic forest zone with a trend of two days per decade (Pulliainen et al., 2017), having a considerable effect on vegetation, but also on wildfire dynamics. At our sites, the length of growing season has a trend of lengthening 4.5-4.8 days per decade and the mean temperature of growing season is increasing by 0.2-0.3°C per decade (SM, Fig. SA2-SA4). Since 1966 the average growing season temperature has increased by approximately 1°C, and the growing season has become longer by approximately 20 days. The cumulative heat index, GDD_5, has increased by 200-300°C days (Fig.4), DI increased from 0.4 to 0.5-0.6 (SM, Fig. SA5). According to the calculated climatic indexes - GDD_5 and DI - conditions throughout the study areas are already suitable for forest and the treeline could have moved to the north. Interestingly, the strongest increase in GDD_5 was observed between years 1966 to 1985, followed by a stable period during the 80s and 90s, and this period was the most favorable to the trees to take over the tundra areas.

Besides atmospheric heat and moisture, Arctic vegetation is sensitive to the state of underlying permafrost. Myers-Smith et al. (2019) emphasized the importance of the increased active layer thickness (ALT) in addition to summer temperature and the elongated growing season for the vegetation shift based on the observations in the Canadian Arctic. They reported a change in a vegetation community composition, namely an increase in shrubs and graminoids, driven by climatic factors alone (see also Barrett et al., 2012; Narita et al., 2015). Tchebakova et al. (2010) suggested that for survival of tree species *Larix siberica* and *Picea obovata*, native to West Siberia, the ALT should exceed 1.5 m. Matyshak et al. (2017b) reported ALT of 58-70 cm in the peatlands near Nadym in 2007-2008, whereas Kukkonen et al. (2020) found ALT of 1-3 m in the nearby boreholes in 2009-2017. Our measurements (Appendix B), although by no means extensive, show that the ALT is 40 cm in the non-disturbed site and 1.5 m in the sites affected by relatively old fires (40 years ago) within study area 1. Due to the changes in surface energy balance, the ALT regularly increases within the first few years following fires (both in forest and tundra ecosystems), and ALT in the burned sites may be larger than in the unburned sites for two or three decades (Rocha and Shaver, 2011; Köster et al., 2018). Deeper ALT provides more space for tree roots, implying more favorable conditions for trees.

In addition, wildfires create new recruitment opportunities (Bret-Harte et al., 2013; Mekonnen et al., 2019). Combusting the vegetation and part of the organic soil layer, the fires create open patches on the soil, where pioneer species can start to grow. Moreover, the burned tundra is darker than the unburned area, which can accelerate tree establishment due to warmer conditions in the soil. This is supported by nutrients released by the burning biomass. Camac et al. (2017) found out that the fires increase shrub seedling survival by as much as 33-fold while warming positively affects their growth rates.

During the latest 60 years, the study sites experienced extensive fires burning 40% of the total territory. The distribution of burned sites among the study areas 1, 2, and 3 was not homogeneous. Within study area 1, a higher fraction of burned areas was detected (Fig. 6). Given the similarity of climatic conditions, a possible explanation is difference in anthropogenic activity. Oil and gas infrastructure within the areas 2 and 3 was launched only recently, whereas geological prospecting within the area 1 started already in 1967, major construction of infrastructures was performed in 1971 and exploitation of Medvezhye field started in 1977. In our analysis of vegetation dynamics, we focused on study area 1 most affected by fires.

It is interesting to note that ca 20% of the burned territories experienced multiple fires with the intervals between consequent fires of 15-60 years. Compared to our results, the fire return interval in Siberian forests at similar latitudes but further to the east (100E), is 130 - 350 years (Kharuk et al., 2011). Note that Kharuk et al. (2011) studied a remote site, where typically lightning ignites a fire. Oppositely, our results suggest that the fire return period in the same latitudes can be significantly reduced, presumably due to anthropogenic influence. Concurrently, this effect could be amplified by higher temperatures and enhanced evaporation. Note that according to Fig. 5, the years of major fires (1976, 1990, 2012 and 2016) were characterized by peaks in potential evapotranspiration, as well as by anomalously high temperature during the growing season (SM, Fig. SA1-SA3) exceeding the mean value by 1°C. Causes of fires in North-West Siberia will be the topic for the future research.

The time since last fire is an important parameter for the assessment of vegetation state. Within the study areas, the interval between the large-scale fire events, when more than 500 km^2 was burned, was 15-25 years. Using the current state of NDVI in the areas affected by fires, we estimated the time of vegetation recovery. The peak NDVI values in the sites that burned 28 years ago (Fig. 7, Table 5) exceeded the peak non-disturbed NDVI value. The peak NDVI value in the sites that burned 2 years ago was smaller than that of the non-disturbed site. This suggests that the post-fire vegetation recovery in our study areas took 2-28 years. Landhausser and Wein (1993) studied recovery of vegetation after the strong fire in the field conditions. Within 5 years after the fire, 65% of the area was not recovered bare ground, but 22 years after the fire the area was fully recovered, which is in general agreement with our results.

The shift of NDVI distribution towards larger NDVI values was found in the sites that burned more than 28 years ago suggesting that recovered vegetation is characterized by a larger amount of biomass, presumably due to the shift in species. Oppositely, lichen does not recover to its state before the fire. The field campaign (Appendix B) revealed an increase of the fraction of green mosses and the tree species (e.g. birch) typical for succession in the burned sites. Increased biomass due to change in vegetation state (increased population of shrubs and forests) after fires is consistent with the other studies (Landhausser and Wein, 1993; Barrett et al., 2012; Narita et al., 2015). Different studies underline bigger post-fire changes in the biomass and composition of the non-vascular plant community in tundra areas (Lantz et al., 2013; Jones et al., 2013), compared to the vascular plant community (Landhausser and Wein, 1993) and in these conditions lichen biomass could take decades to centuries to recover.

Our results (sec. 3.3) suggest that the disturbances have an important effect on the forest advance. We observed an increase in the forest and woodland cover in the areas affected by relatively 'old' fires (60 years period). In undisturbed conditions, forest took over tundra vegetation on the slopes and in the river valleys. As tundra turned into woodlands on rather moderate slopes (3 degrees), it is not likely that landslides played a definitive role. Instead, the vegetation shift may be related to the difference in insolation or hydrological regime (Walvoord et al., 2019). Frost and Epstein (2014) studied expansion of larch and tall shrubs in Siberia based on remote sensing. The expansion of trees and shrubs was observed in uplands, which were defined as the sites with topographic slopes above 2 degrees. This is in agreement with our findings. Notably, the topography was not an important factor for the vegetation shift in the fire-affected areas.

5 Conclusions

We used topographic maps and high-resolution remote sensing to study vegetation dynamics in the forest-tundra zone of North-West Siberia during the last 60 years. We found that the vegetation shift from dry tundra to forest was strongly associated with fires. In the non-disturbed sites experiencing no fires, only 6% of the area in southern tundra developed some trees during the 60-year period. This number increased up to 15% of the area in the forest-tundra ecotone and northern taiga. The shift in the non-disturbed area was sensitive to topography, and trees appeared mainly on the moderate slopes. In the fire-affected sites, after the same period, the tree-dominated vegetation occupied already 40-85% of the previous dry tundra in the forest-tundra ecotone and northern taiga.

Given the importance of the fires for the tundra-forest dynamics, we calculated fire frequency within the study area. The major fires, burning 600 – 2500 km^2 of the study area, occurred every 15-25 years. Most of the burned area experienced fires only once during 60 years, although some parts experienced multiple burning, up to 4 times. For ca 1700 km^2 of the study area, the period between the consequent fires is rather short, ca 15-60 years. This was a much shorter period compared to the neighboring remote sites of Central Siberia (fire return period longer than 100 years) that are less affected by anthropogenic influence.

Monitoring of wildfires in Russia is focused on forests whereas importance of tundra fires is underestimated. This is a major overlook which might have great economic consequences taking into account that tundra fires further decrease pasture areas for reindeer, already extremely overused in North-West Siberia (by 100-150% on Yamal and Gydan peninsulas according to Matveev and Musaev, 2013). In our study sites, the fires burned half of the dry tundra (6000 km^2) in 60 years. As concluded from our analysis, most of these areas likely shifted or will shift to woodlands and forests.

Converting the tundra to dark needle leaved forest causes an energy balance shift where especially areas with spruce have a positive (warming) feedback to climate in the future. Decrease in albedo causes increase of energy input to the surface, and partitioning of energy shifts towards sensible heat flux at forested sites (Beringer et al., 2005).

On the positive side, increase of forest areas may give a hint to enhancement of carbon sink and accordingly also of Carbon-Sink+ (Kalliokoski et al., 2019). Overall, the importance and need of detailed comprehensive long-term data is also obvious, therefore it is important to complete and verify satellite remote sensing data by observations – to establish Station for Measuring Earth surface – Atmosphere Relations (SMEAR) (Kulmala, 2018) in North-West Siberia as a part of Pan-Eurasian Experiment (PEEX) activities (Kulmala et al., 2015; Lappalainen et al., 2016; Petäjä et al., 2020).

Code and data availability. Meteorological data are available on the following website: http://meteo.ru. Study areas, reference sites, burned areas and control points for vegetation change can be found in geoportal NC50 (https://ageoportal.ipos-tmn.ru/nadym/). Other data sets are available from the authors upon request.

Appendix A: Description of geoportal ‘Nadym. Changes in 50 years (1968-2018)’ (NC50)

The geoportal ‘Nadym. Changes in 50 years (1968-2018)’ (NC50), available at https://ageoportal.ipos-tmn.ru/nadym/, aims to provide detailed geographical information on the study sites. There are three maps in geoportal NC50 (Fig. A1). The maps are synchronized, i.e. zoom or pan in one of the maps results in the same operation in two other maps. Each map contains a pointer in the center.

1) Map 1 is constructed of Corona/KH-4b imagery with marked study areas and reference sites. In the upper left corner, there are zoom instruments. In the upper right corner, there is a widget containing bookmarks of the reference sites. The reference sites are marked by yellow polygons in the map 1.

2) Map 2 is constructed of super high-resolution imagery: Yandex Maps, Bing Maps or Global Forest Watch. Fire-affected areas from different years can be overlain on this map. In addition, the field of Map 2 can be used to check the vegetation change in the control points. In the upper right corner, there is a panel of map layers.

3) Map 3 can be used as a digital elevation map (ArcticDEM) or a topographic map. In the upper right corner, there is a panel of map layers and coordinates of the pointer position (degrees-minutes-seconds). The coordinates in the decimal format are copied to the clipboard by a mouse click.

Appendix B: In-situ observations of vegetation and permafrost state

In August 2019, a field campaign was performed near Pangody in the central part of study area 1 (Fig. 1) to study vegetation cover and state of permafrost. We chose three sites: one in the non-disturbed area, one in the area burned before 1968 and one in the area burned in 1968 and 1988. Photos from two of them are shown in Fig. B1. The land cover of each site consisted mainly of mosses, grasses and shrubs (detailed classification is given in Table B1), and the major tree species were larix and spruce (*Larix sibirica, Picea obovata*). In the burned sites, birch (*Betula pubescens*) and pine (*Pinus Sylvestris L., Pinus sibirica*) were also observed.

The active layer thickness (the depth of annual thaw) was measured using a metal rod: the rod was pushed vertically into the ground until it reached frozen soil. Active layer thickness (ALT) for three sites is reported in Table B1.

Author contributions. EE, OS and KK designed and conceptualized the study. OS processed satellite data (mosaics, classification). OS and PT developed the geoportal, analyzed the data, prepared figures and interpreted results. NP performed on-site data acquisition. EE analysed data (meteo, NDVI), prepared figures, interpreted results and wrote the manuscript. KK interpreted results and contributed to writing discussion. AS, KK, JB, TP, SZ and MK contributed with data interpretation and writing - review and editing. All the authors commented on the manuscript.

Competing interests. The authors declare that they have no conflict of interest.

Acknowledgements. EE and TP acknowledge Academy of Finland Center of Excellence program (grant no. 307331) and Belmont Forum project Arctic Community Resilience to Boreal Environmental change: Assessing Risks from fire and disease (ACRoBEAR) via Academy of Finland, decision number 334792. OS and AS were funded by RFBR, research project 20-55-71004 and Belmont Forum project 1729 SERUS. PT was funded by Russian Science Foundation project 18-17-00178. MK acknowledges the Academy of Finland professor grant (no. 302958) and ATM-GTP European Research Council grant under the European Union's Horizon 2020 research and innovation program (no. 742206). OS, AS, SZ and JB acknowledge bilateral collaboration supported by Academy of Finland grant 314 798/799 and Russian Foundation for Basic Research grants 18-55-11005 and 19-17-00209. TP acknowledges Funding through Academy of Finland ('Natural Secreted Nano Vesicles as a Source of Novel Biomass Products for Circular Economy', NANOBIOMASS, 307537) and the European Union's Horizon 2020 research and innovation program under grant agreement No 689443 via project iCUPE (Integrative and Comprehensive Understanding on Polar Environments). KK was supported by the Academy of Finland (Academy Research Fellow project 294600).

References

Aakala, T., Hari, P., Dengel, S., Newberry, S. L., Mizunuma, T., and Grace, J.: A prominent stepwise advance of the tree line in north-east Finland, Journal of Ecology, 102, 1582–1591, 2014.

Barrett, K., Rocha, A. V., van de Weg, M. J., and Shaver, G.: Vegetation shifts observed in arctic tundra 17 years after fire, Remote Sensing Letters, 3, 729–736, 2012.

Beringer, J., Chapin III, F. S., Thompson, C. C., and McGuire, A. D.: Surface energy exchanges along a tundra-forest transition and feedbacks to climate, Agricultural and Forest Meteorology, 131, 143–161, 2005.

Bernes, C., Bråthen, K. A., Forbes, B. C., Speed, J. D., and Moen, J.: What are the impacts of reindeer/caribou (Rangifer tarandus L.) on arctic and alpine vegetation? A systematic review, Environmental Evidence, 4, 4, 2015.

Bjorkman, A. D., Criado, M. G., Myers-Smith, I. H., Ravolainen, V., Jónsdóttir, I. S., Westergaard, K. B., Lawler, J. P., Aronsson, M., Bennett, B., Gardfjell, H., et al.: Status and trends in Arctic vegetation: Evidence from experimental warming and long-term monitoring, Ambio, 49, 678–692, 2020.

Blaschke, T.: Object based image analysis for remote sensing, ISPRS journal of photogrammetry and remote sensing, 65, 2–16, 2010.

Bonan, G. B.: A computer model of the solar radiation, soil moisture, and soil thermal regimes in boreal forests, Ecological Modelling, 45, 275–306, 1989.

Box, J. E., Colgan, W. T., Christensen, T. R., Schmidt, N. M., Lund, M., Parmentier, F.-J. W., Brown, R., Bhatt, U. S., Euskirchen, E. S., Romanovsky, V. E., et al.: Key indicators of Arctic climate change: 1971–2017, Environmental Research Letters, 14, 045 010, 2019.

Bret-Harte, M. S., Mack, M. C., Shaver, G. R., Huebner, D. C., Johnston, M., Mojica, C. A., Pizano, C., and Reiskind, J. A.: The response of Arctic vegetation and soils following an unusually severe tundra fire, Philosophical Transactions of the Royal Society B: Biological Sciences, 368, 20120 490, 2013.

Camac, J. S., Williams, R. J., Wahren, C.-H., Hoffmann, A. A., and Vesk, P. A.: Climatic warming strengthens a positive feedback between alpine shrubs and fire, Global Change Biology, 23, 3249–3258, 2017.

Chorley, R. J.: Introduction to physical hydrology, London: Methuen, 1971.

Frost, G. V. and Epstein, H. E.: Tall shrub and tree expansion in Siberian tundra ecotones since the 1960s, Global Change Biology, 20, 1264–1277, 2014.

Hansen, M. C., Potapov, P. V., Moore, R., Hancher, M., Turubanova, S. A., Tyukavina, A., Thau, D., Stehman, S., Goetz, S. J., Loveland, T. R., et al.: High-resolution global maps of 21st-century forest cover change, Science, 342, 850–853, 2013.

Harsch, M. A. and Bader, M. Y.: Treeline form–a potential key to understanding treeline dynamics, Global Ecology and Biogeography, 20, 582–596, 2011.

Ilyina, I. S., Lapshina, E. I., Lavrenko, N. N., et al.: West Siberian Plain Vegetation Cover, 1985.

Johansen, B. and Tømmervik, H.: The relationship between phytomass, NDVI and vegetation communities on Svalbard, International Journal of Applied Earth Observation and Geoinformation, 27, 20–30, 2014.

Joly, K., Jandt, R. R., and Klein, D. R.: Decrease of lichens in Arctic ecosystems: the role of wildfire, caribou, reindeer, competition and climate in north-western Alaska, Polar Research, 28, 433–442, 2009.

Jones, B. M., Breen, A. L., Gaglioti, B. V., Mann, D. H., Rocha, A. V., Grosse, G., Arp, C. D., Kunz, M. L., and Walker, D. A.: Identification of unrecognized tundra fire events on the north slope of Alaska, Journal of Geophysical Research: Biogeosciences, 118, 1334–1344, 2013.

Kalliokoski, T., Aalto, T., Bäck, J., Ezhova, E., Franz, D., Haapanala, S., Juurola, E., Kerminen, V.-M., Kolari, P., Kulmala, L., et al.: Carbon sink and CarbonSink+: from observations to global potential, 2019.

Kaplan, J. O. and New, M.: Arctic climate change with a 2°C global warming: Timing, climate patterns and vegetation change, Climatic change, 79, 213–241, 2006.

Katsov, V., Semenov, S., Alekseev, G., Ananicheva, M., et al.: Second Roshydromet Assessment Report on Climate Change and its Consequences in the Russian Federation, Moscow, Roshydromet, 2014.

Kharuk, V. I., Ranson, K. J., Dvinskaya, M. L., and Im, S. T.: Wildfires in northern Siberian larch dominated communities, Environmental Research Letters, 6, 045 208, 2011.

Köster, E., Köster, K., Aurela, M., Laurila, T., Berninger, F., Lohila, A., and Pumpanen, J.: Impact of reindeer herding on vegetation biomass and soil carbon content: a case study from Sodankylä, Finland., Boreal Environment Research, 2013.

Köster, E., Köster, K., Berninger, F., Prokushkin, A., Aaltonen, H., Zhou, X., and Pumpanen, J.: Changes in fluxes of carbon dioxide and methane caused by fire in Siberian boreal forest with continuous permafrost, Journal of environmental management, 228, 405–415, 2018.

Kukkonen, I. T., Suhonen, E., Ezhova, E., Lappalainen, H., Gennadinik, V., Ponomareva, O., Gravis, A., Miles, V., Kulmala, M., Melnikov, V., et al.: Observations and modelling of ground temperature evolution in the discontinuous permafrost zone in Nadym, north-west Siberia, Permafrost and Periglacial Processes, 2020.

Kulmala, M.: Build a global Earth observatory, Nature, 553, 21–23, 2018.

Kulmala, M., Nieminen, T., Chellapermal, R., Makkonen, R., Bäck, J., and Kerminen, V.-M.: Climate feedbacks linking the increasing atmospheric CO_2 concentration, BVOC emissions, aerosols and clouds in forest ecosystems, in: Biology, controls and models of tree volatile organic compound emissions, pp. 489–508, Springer, 2013.

Kulmala, M., Lappalainen, H. K., Petäjä, T., Kurten, T., Kerminen, V.-M., Viisanen, Y., Hari, P., Sorvari, S., Bäck, J., Bondur, V., Kasimov, N., Kotlyakov, V., Matvienko, G., Baklanov, A., Guo, H. D., Ding, A., Hansson, H.-C., and Zilitinkevich, S.: Introduction: The Pan-Eurasian Experiment (PEEX) - multidisciplinary, multiscale and multicomponent research and capacity-building initiative, Atmospheric Chemistry and Physics, 15, 13 085–13 096, https://doi.org/10.5194/acp-15-13085-2015, https://www.atmos-chem-phys.net/15/13085/2015/, 2015.

Kulmala, M., Ezhova, E., Kalliokoski, T., Noe, S., Vesala, T., Lohila, A., Liski, J., Makkonen, R., Bäck, J., Petäjä, T., and Kerminen, V.-M.: CarbonSink+ — Accounting for multiple climate feedbacks from forests, Boreal Environment Research, 25, 145–159, 2020.

Landhausser, S. M. and Wein, R. W.: Postfire vegetation recovery and tree establishment at the Arctic treeline: climate-change-vegetation-response hypotheses, Journal of Ecology, pp. 665–672, 1993.

Lantz, T. C., Marsh, P., and Kokelj, S. V.: Recent shrub proliferation in the Mackenzie Delta uplands and microclimatic implications, Ecosystems, 16, 47–59, 2013.

Lappalainen, H. K., Kerminen, V.-M., Petäjä, T., Kurten, T., Baklanov, A., Shvidenko, A., Bäck, J., Vihma, T., Alekseychik, P., Andreae, M. O., Arnold, S. R., Arshinov, M., Asmi, E., Belan, B., Bobylev, L., Chalov, S., Cheng, Y., Chubarova, N., de Leeuw, G., Ding, A., Dobrolyubov, S., Dubtsov, S., Dyukarev, E., Elansky, N., Eleftheriadis, K., Esau, I., Filatov, N., Flint, M., Fu, C., Glezer, O., Gliko, A., Heimann, M., Holtslag, A. A. M., Hõrrak, U., Janhunen, J., Juhola, S., Järvi, L., Järvinen, H., Kanukhina, A., Konstantinov, P., Kotlyakov, V., Kieloaho, A.-J., Komarov, A. S., Kujansuu, J., Kukkonen, I., Duplissy, E.-M., Laaksonen, A., Laurila, T., Lihavainen, H., Lisitzin, A., Mahura, A., Makshtas, A., Mareev, E., Mazon, S., Matishov, D., Melnikov, V., Mikhailov, E., Moisseev, D., Nigmatulin, R., Noe, S. M., Ojala, A., Pihlatie, M., Popovicheva, O., Pumpanen, J., Regerand, T., Repina, I., Shcherbinin, A., Shevchenko, V., Sipilä, M., Skorokhod, A., Spracklen, D. V., Su, H., Subetto, D. A., Sun, J., Terzhevik, A. Y., Timofeyev, Y., Troitskaya, Y., Tynkkynen, V.-P., Kharuk, V. I., Zaytseva, N., Zhang, J., Viisanen, Y., Vesala, T., Hari, P., Hansson, H. C., Matvienko, G. G., Kasimov, N. S., Guo, H., Bondur, V., Zilitinkevich, S., and Kulmala, M.: Pan-Eurasian Experiment (PEEX): towards a holistic understanding of the feedbacks and interactions in the land–atmosphere–ocean–society continuum in the northern Eurasian region, Atmospheric Chemistry and Physics, 16, 14 421–14 461, https://doi.org/10.5194/acp-16-14421-2016, 2016.

MacDonald, G., Kremenetski, K., and Beilman, D.: Climate change and the northern Russian treeline zone, Philosophical Transactions of the Royal Society B: Biological Sciences, 363, 2283–2299, 2008.

Maliniemi, T., Kapfer, J., Saccone, P., Skog, A., and Virtanen, R.: Long-term vegetation changes of treeless heath communities in northern Fennoscandia: Links to climate change trends and reindeer grazing, Journal of Vegetation Science, 29, 469–479, 2018.

Matveev, A. A. and Musaev, R. A.: Preservation of the ecological balance in the context of the economic development of Yamal-Nenets Autonomous district, in: Proceedings of the international conference 'Economy and modern Management: Theory and Practice', p. 33436, Novosibirsk, 2013.

Matyshak, G., Bogatyrev, L., Goncharova, O. Y., and Bobrik, A.: Specific features of the development of soils of hydromorphic ecosystems in the northern taiga of Western Siberia under conditions of cryogenesis, Eurasian Soil Science, 50, 1115–1124, 2017a.

Matyshak, G., Goncharova, O. Y., Moskalenko, N., Walker, D., Epstein, H., and Shur, Y.: Contrasting soil thermal regimes in the Forest-tundra transition near Nadym, West Siberia, Russia, Permafrost and Periglacial Processes, 28, 108–118, 2017b.

Mekonnen, Z. A., Riley, W. J., Randerson, J. T., Grant, R. F., and Rogers, B. M.: Expansion of high-latitude deciduous forests driven by interactions between climate warming and fire, Nature plants, 5, 952–958, 2019.

Miles, V. V. and Esau, I.: Spatial heterogeneity of greening and browning between and within bioclimatic zones in northern West Siberia, Environmental Research Letters, 11, 115 002, 2016.

Myers-Smith, I. H. and Hik, D. S.: Climate warming as a driver of tundra shrubline advance, Journal of Ecology, 106, 547–560, 2018.

Myers-Smith, I. H., Grabowski, M. M., Thomas, H. J., Angers-Blondin, S., Daskalova, G. N., Bjorkman, A. D., Cunliffe, A. M., Assmann, J. J., Boyle, J. S., McLeod, E., et al.: Eighteen years of ecological monitoring reveals multiple lines of evidence for tundra vegetation change, Ecological Monographs, 89, e01 351, 2019.

Myers-Smith, I. H., Kerby, J. T., Phoenix, G. K., Bjerke, J. W., Epstein, H. E., Assmann, J. J., John, C., Andreu-Hayles, L., Angers-Blondin, S., Beck, P. S., et al.: Complexity revealed in the greening of the Arctic, Nature Climate Change, 10, 106–117, 2020.

Narita, K., Harada, K., Saito, K., Sawada, Y., Fukuda, M., and Tsuyuzaki, S.: Vegetation and permafrost thaw depth 10 years after a tundra fire in 2002, Seward Peninsula, Alaska, Arctic, Antarctic, and Alpine Research, 47, 547–559, 2015.

Olofsson, J., Oksanen, L., Callaghan, T., Hulme, P. E., Oksanen, T., and Suominen, O.: Herbivores inhibit climate-driven shrub expansion on the tundra, Global Change Biology, 15, 2681–2693, 2009.

Petäjä, T., Ganzei, K., Lappalainen, H. K., Tabakova, K., Makkonen, R., Räisänen, J., Chalov, S., Kulmala, M., Zilitinkevich, S., Baklanov, P., Shakirov, R. B., Mishina, N. V.and Egidarev, E. G., and Kondrat'ev, I. I.: Research agenda for the Russian Far East and utilization of multi-platform comprehensive environmental observations, Int. J. Digital Earth, submitted, 2020.

Ponomarev, E. I., Kharuk, V. I., and Ranson, K. J.: Wildfires dynamics in Siberian larch forests, Forests, 7, 125, 2016.

Post, E. and Pedersen, C.: Opposing plant community responses to warming with and without herbivores, Proceedings of the National Academy of Sciences, 105, 12 353–12 358, 2008.

Priestley, C. H. B. and Taylor, R.: On the assessment of surface heat flux and evaporation using large-scale parameters, Monthly weather review, 100, 81–92, 1972.

Pulliainen, J., Aurela, M., Laurila, T., Aalto, T., Takala, M., Salminen, M., Kulmala, M., Barr, A., Heimann, M., Lindroth, A., et al.: Early snowmelt significantly enhances boreal springtime carbon uptake, Proceedings of the National Academy of Sciences, 114, 11 081–11 086, 2017.

Renwick, K. M. and Rocca, M. E.: Temporal context affects the observed rate of climate-driven range shifts in tree species, Global Ecology and Biogeography, 24, 44–51, 2015.

Rocha, A. V. and Shaver, G. R.: Postfire energy exchange in arctic tundra: the importance and climatic implications of burn severity, Global Change Biology, 17, 2831–2841, 2011.

Ruffner, K. C.: Corona: America's first satellite program, History Staff, Center for the Study of Intelligence, Central Intelligence Agency, 1995.

Sand, M., Berntsen, T., von Salzen, K., Flanner, M., Langner, J., and Victor, D. G.: Response of Arctic temperature to changes in emissions of short-lived climate forcers, Nature Climate Change, 6, 286–289, 2016.

Sannikov, S. et al.: Survival and growth of seedlings of conifer species in different types of micro-environment on felled areas., Ekologiya, pp. 60–68, 1970.

Sizov, O. S. and Lobotrosova, S. A.: Features of revegetation of sand blowout sites in the northern taiga subzone of Western Siberia, Earth Cryosphere, XX, 3–13, 2016.

Tchebakova, N. M., Monserud, R. A., and Nazimova, D. I.: A Siberian vegetation model based on climatic parameters, Canadian Journal of Forest Research, 24, 1597–1607, 1994.

Tchebakova, N. M., Parfenova, E. I., and Soja, A. J.: Potential climate-induced vegetation change in Siberia in the twenty-first century, in: Environmental Change in Siberia, pp. 67–82, Springer, 2010.

Trofimova, I. E. and Balybina, A. S.: Regionalization of the West Siberian Plain from thermal regime of soils, Geography and Natural Resources, 36, 234–244, 2015.

Van Bogaert, R., Haneca, K., Hoogesteger, J., Jonasson, C., De Dapper, M., and Callaghan, T. V.: A century of tree line changes in sub-Arctic Sweden shows local and regional variability and only a minor influence of 20th century climate warming, Journal of Biogeography, 38, 907–921, 2011.

Vermote, E., Justice, C., Claverie, M., and Franch, B.: Preliminary analysis of the performance of the Landsat 8/OLI land surface reflectance product, Remote Sensing of Environment, 185, 46–56, 2016.

Walker, D., Epstein, H., Jia, G., Balser, A., Copass, C., Edwards, E., Gould, W., Hollingsworth, J., Knudson, J., Maier, H., et al.: Phytomass, LAI, and NDVI in northern Alaska: Relationships to summer warmth, soil pH, plant functional types, and extrapolation to the circumpolar Arctic, Journal of Geophysical Research: Atmospheres, 108, 2003.

Walker, D. A., Raynolds, M. K., Daniëls, F. J., Einarsson, E., Elvebakk, A., Gould, W. A., Katenin, A. E., Kholod, S. S., Markon, C. J., Melnikov, E. S., et al.: The circumpolar Arctic vegetation map, Journal of Vegetation Science, 16, 267–282, 2005.

Walvoord, M. A., Voss, C. I., Ebel, B. A., and Minsley, B. J.: Development of perennial thaw zones in boreal hillslopes enhances potential mobilization of permafrost carbon, Environmental Research Letters, 14, 015 003, 2019.

Woodward, F. I., Lomas, M. R., and Kelly, C. K.: Global climate and the distribution of plant biomes, Philosophical Transactions of the Royal Society of London. Series B: Biological Sciences, 359, 1465–1476, 2004.

Wulder, M. A., Loveland, T. R., Roy, D. P., Crawford, C. J., Masek, J. G., Woodcock, C. E., Allen, R. G., Anderson, M. C., Belward, A. S., Cohen, W. B., et al.: Current status of Landsat program, science, and applications, Remote sensing of environment, 225, 127–147, 2019.

Zhu, K., Woodall, C. W., and Clark, J. S.: Failure to migrate: lack of tree range expansion in response to climate change, Global Change Biology, 18, 1042–1052, 2012.

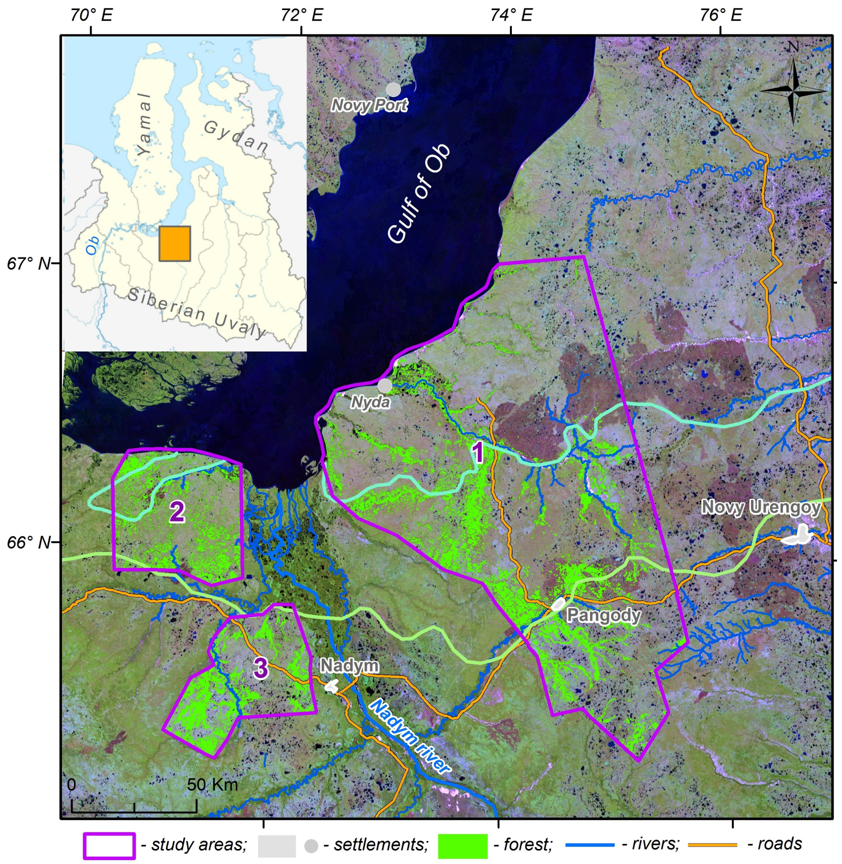

Figure 1. Study areas 1, 2 and 3 are shown in the Landsat -8 mosaic (2018). Green areas display the forest mask obtained from the topographic map (Ilyina et al., 1985). Cyan curve is the boundary between southern tundra and tundra-forest ecotone, light green curve is the boundary between forest-tundra ecotone and northern taiga (Ilyina et al., 1985). Inset: orange rectangular region marks the location of the study sites on the map of Yamal-Nenets Autonomous District.

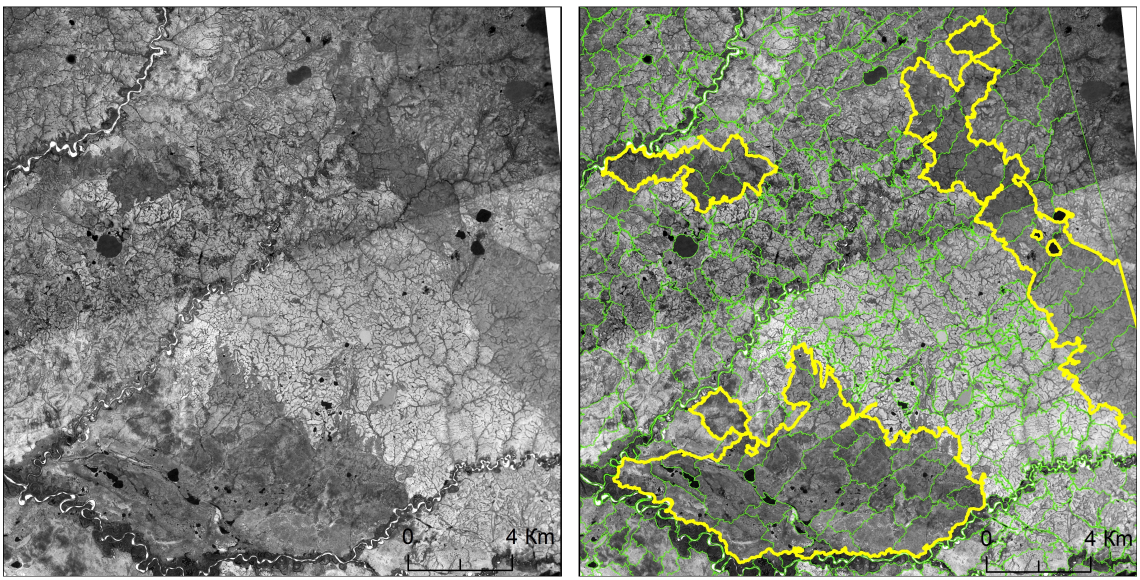

Figure 2. An example of segmentation and classification of burned areas in Corona mosaic. Left panel: original mosaic. Right panel: mosaic after segmentation and classification. Green curves - boundaries of segments, yellow curves - boundaries of identified burned areas.

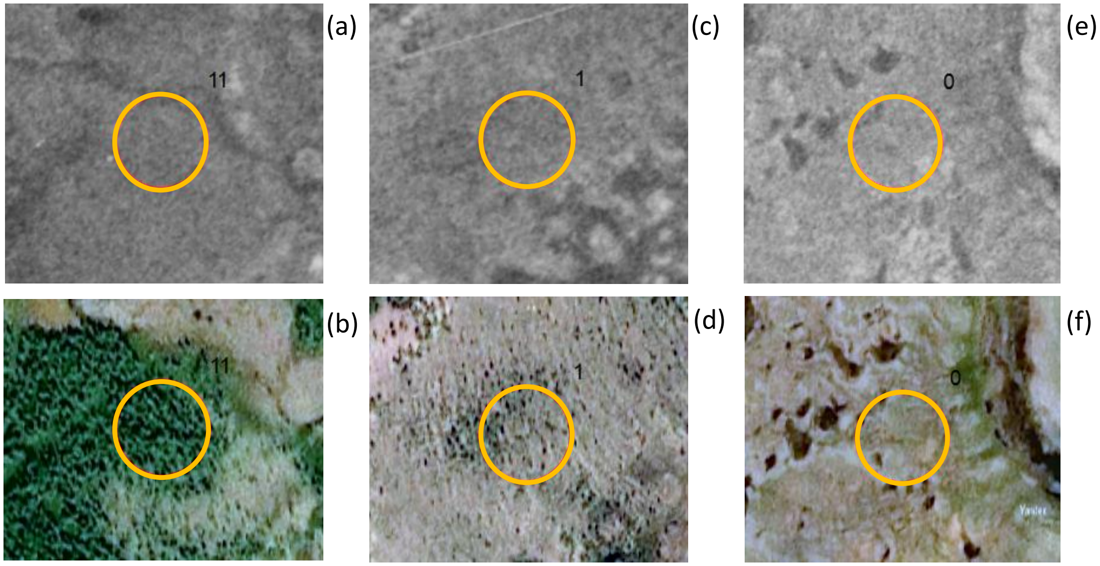

Figure 3. Examples of samples used for the visual analysis of vegetation dynamics. Diameter of each sample is 100 m. The images are taken from Corona and SPOT-6,7 mosaic (©Yandex.Maps). (a)-(b): shift to forest, (c)-(d): shift to woodlands, (e)-(f): no shift.

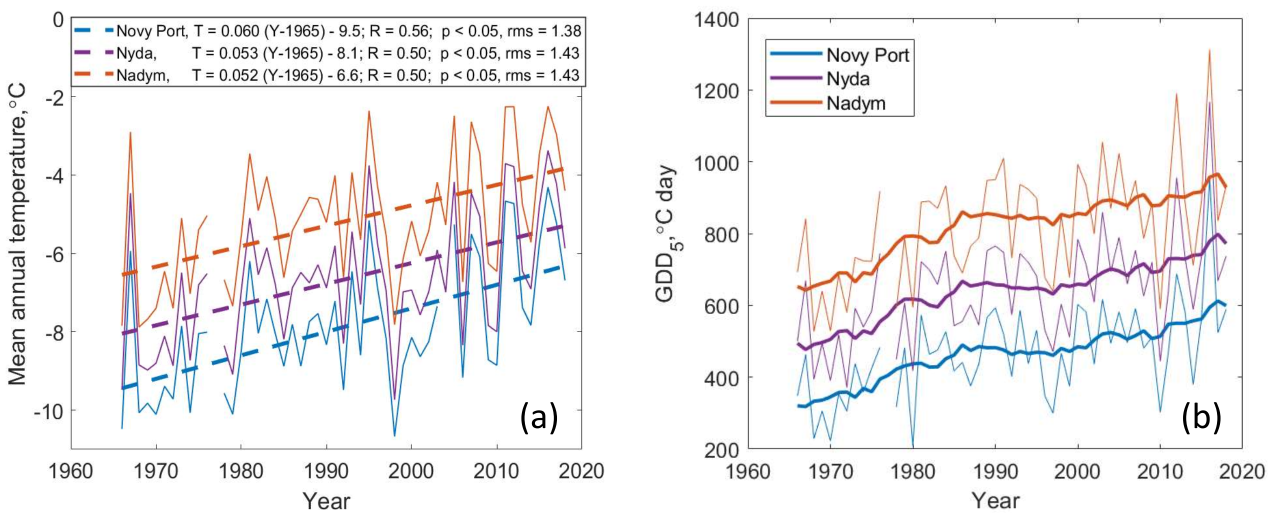

Figure 4. (a) Time series of mean annual temperature (solid) and corresponding linear fits (dashed). In the legend, T is the mean annual temperature and Y is the year. (b) Time series of growing degree-days (thin solid curves) and 10-yr running average (thick solid curves)

.

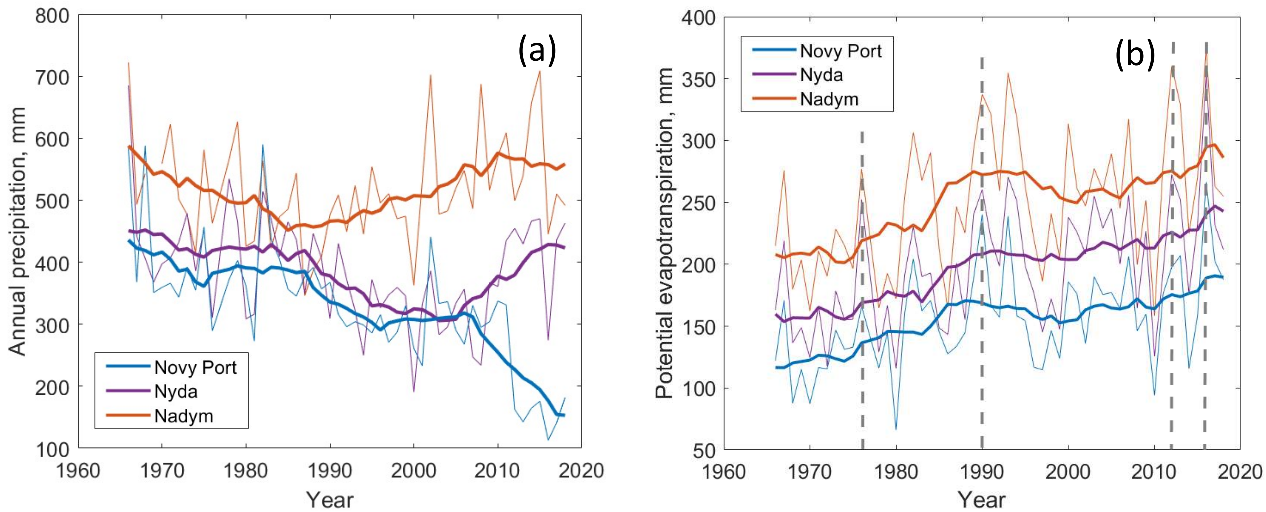

Figure 5. (a) Time series of annual precipitation and (b) potential evapotranspiration. Thick curves correspond to 10-yr running average. Dashed lines in panel (b) mark the years of major fires.

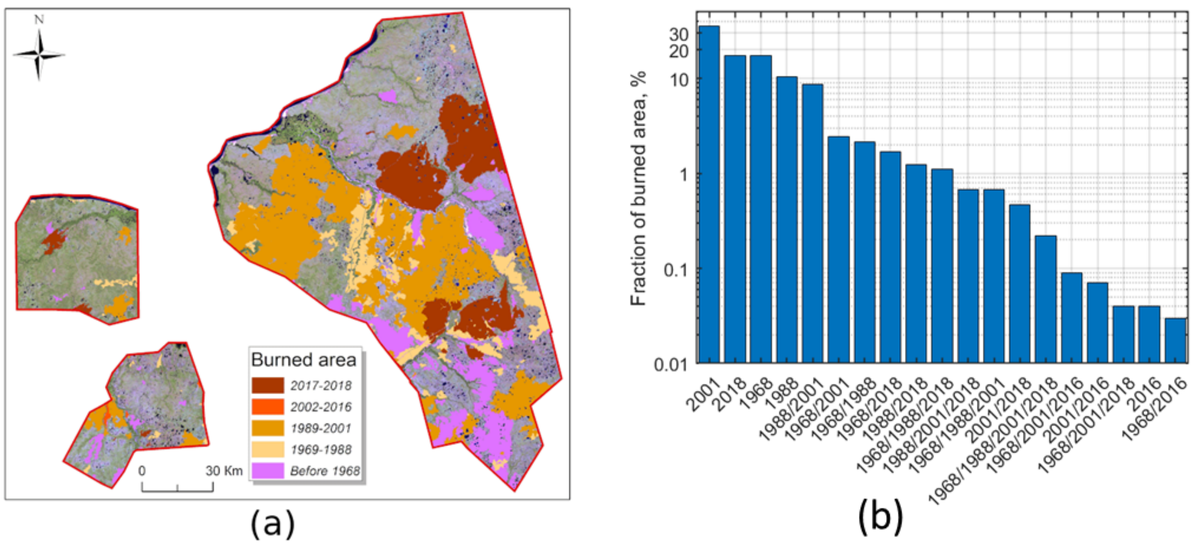

Figure 6. (a) Burned territories within study areas 1, 2 and 3 shown in Landsat-8 mosaic (2018). Dates in the legend correspond to different fire periods or different major fires. (b) The fraction of burned area defined as the burned area in the mosaic from particular year(s) divided by the total burned area during the whole study period. Each year marks the end of the corresponding period mentioned in Fig.6a. Multiple years in x-axis correspond to multiple fires at the same site.

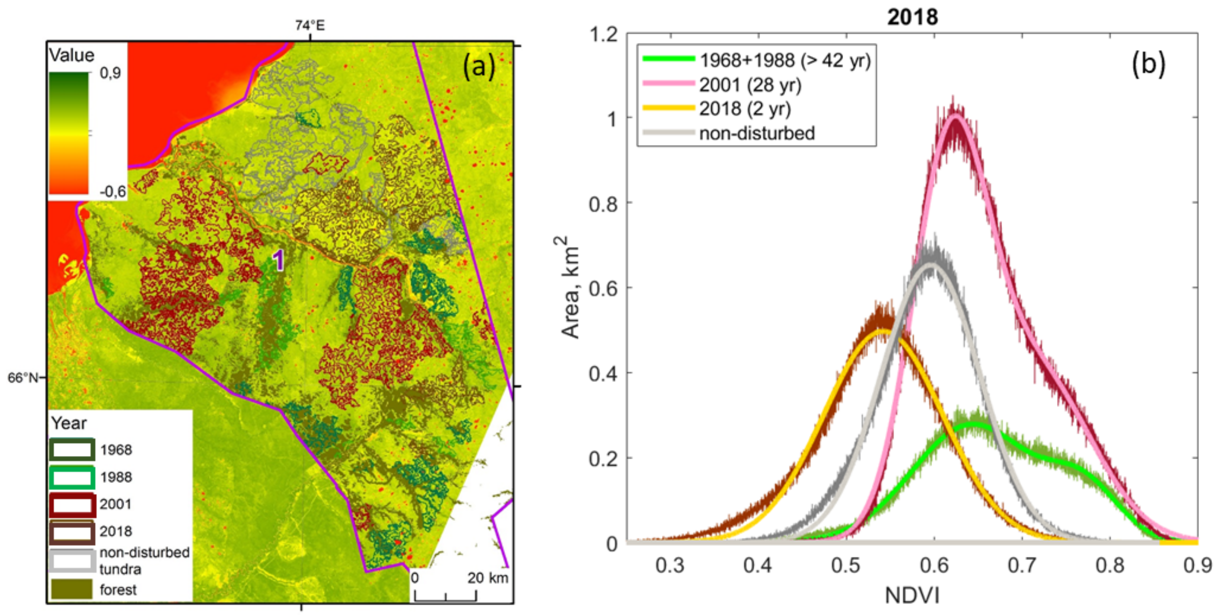

Figure 7. (a) The distribution of NDVI over study area 1 on 30 June 2018. Segments with boundaries of different color are non-disturbed dry tundra sites and burned dry tundra sites detected in Corona and Landsat mosaics from different years (see legend). Burned areas in the mosaics from 1968 and 1988 are mainly due to fires from >42 years ago, in 2001 – due to fires from 28 years ago, in 2018 – due to fires from 2 years ago. (b) Distributions of NDVI based on the data from marked non-disturbed sites and sites burned in different years. In the legend, numbers in brackets indicate years after the last major fire.

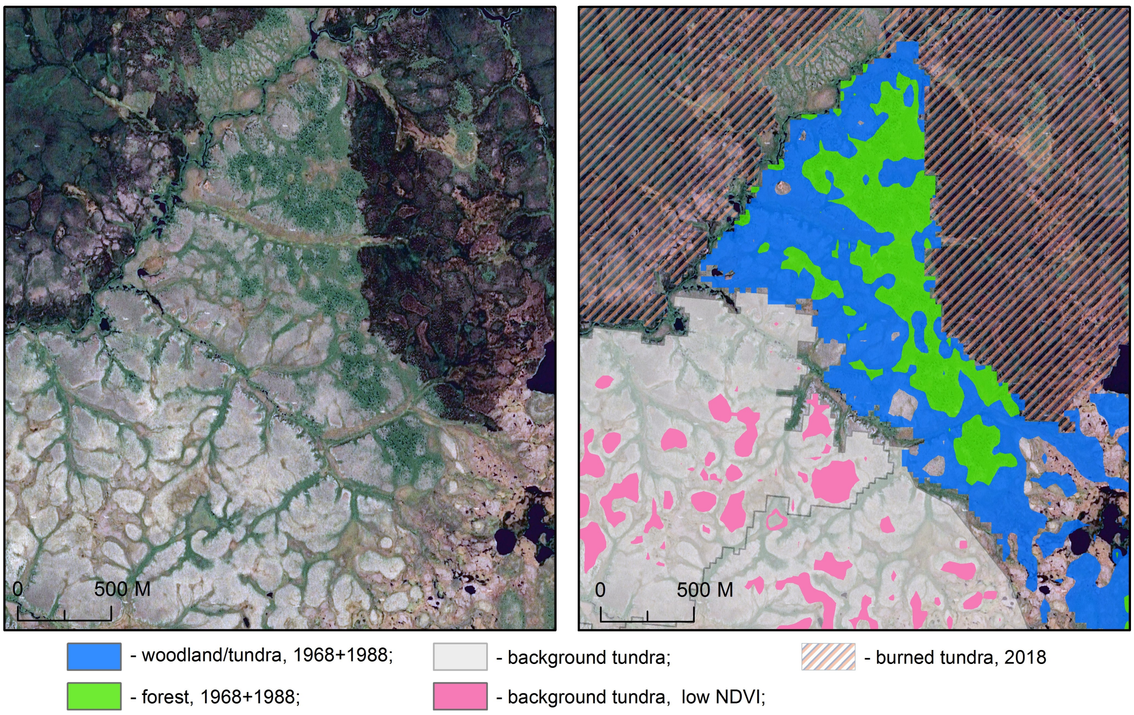

Figure 8. Representative types of vegetation associated with different state of the sites and NDVI. Left panel: an image without mask, right panel: the same image colored according to the state of the site (burned in mosaics from 1968+1988 or 2018, non-disturbed) and to NDVI. Right panel: green color corresponds to the upper peak and blue color corresponds to the lower peak in the bimodal distribution from the sites burned before 1968 and 1988 (Fig. 7b). Pink color marks areas with NDVI lower than 0.52 in the non-disturbed site.

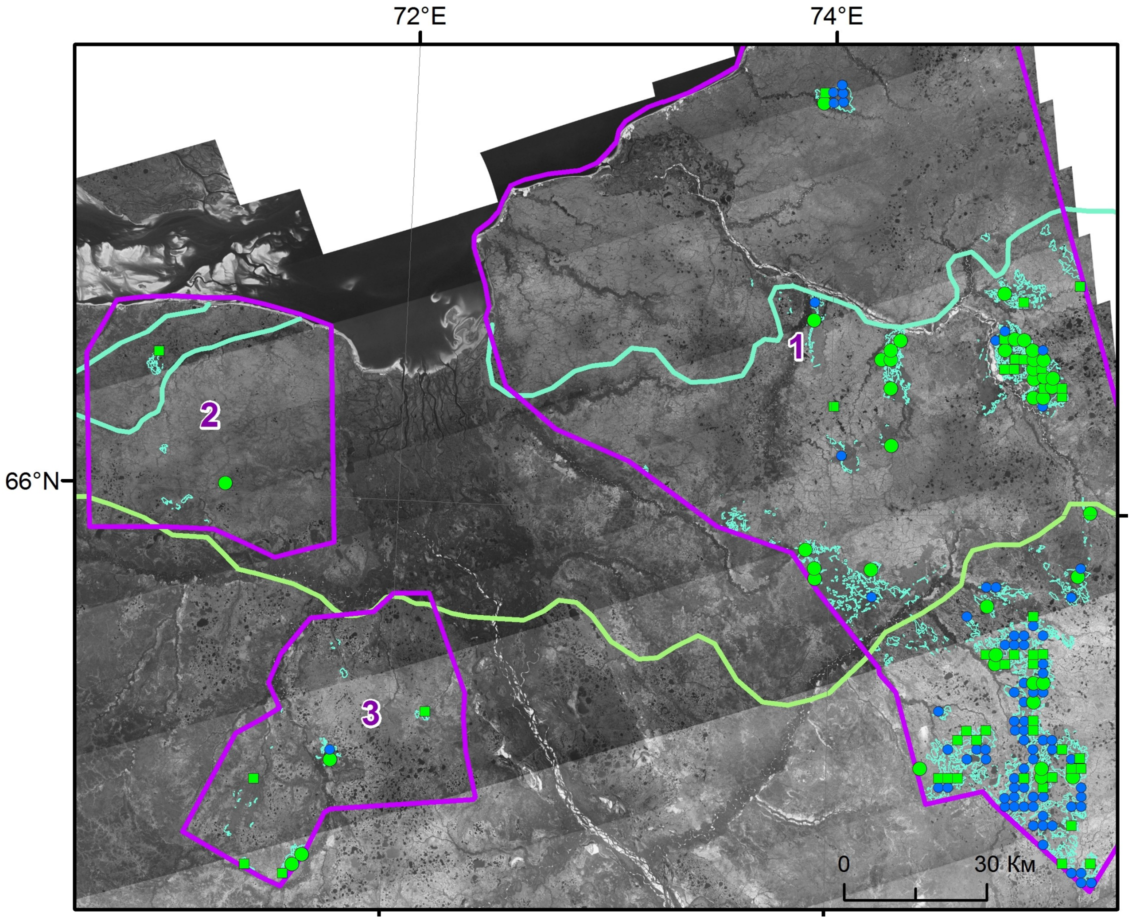

Figure 9. Illustration of the vegetation shift in dry tundra after the fire (time interval ca 60 years). Blue circles – no shift, green squares – shift to woodlands, green circles – shift to forest. Cyan curve is the boundary between southern tundra and forest-tundra, green curve is the boundary between forest-tundra and northern taiga (source: topographic maps).

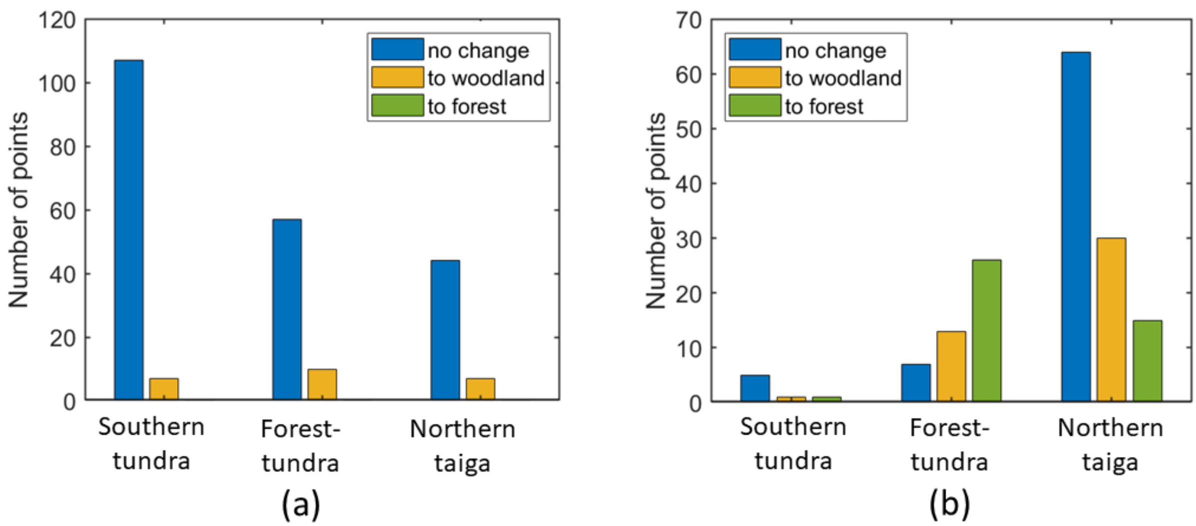

Figure 10. Number of checkpoints corresponding to different classes of vegetation type change for three vegetation zones: (a) non-disturbed territories, (b) fire-affected territories. Change classes: 'no change' means that tundra was both in the old and modern images, 'to woodland' means that tundra turned to woodland and 'to forest' means that tundra turned to forest. Vegetation zones (southern tundra, forest-tundra and northern taiga) are based on topographic maps (Fig. 9). The time interval is ca 60 years.

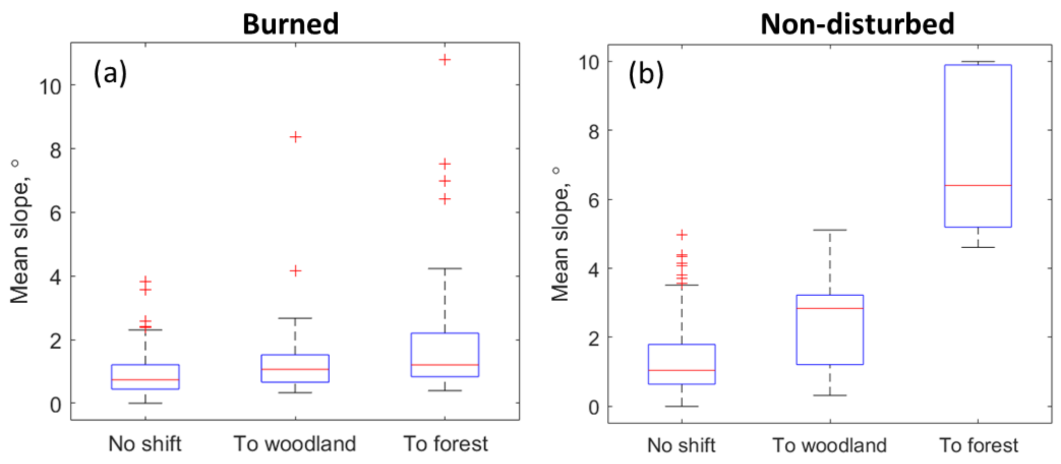

Figure 11. Median boxplots of the mean topographic slopes within the check circles. Red line - median values, bottom and top edges of boxes – 25th and 75th percentiles, whiskers 5th and 95th percentiles and red crosses - outliers.

Table 1. Description of the study areas. Classification of the study areas according to vegetation types.

Study area	Location	Surface area (km^2)	Vegetation distribution (Ilyina et al., 1985)
1	triangle with vertices at (65°17'N 75°12'E), (66°30'N 72°05'E) and (67°06'N 74°40'E)	15800	ca 50% of dry and wet tundra (mainly northern part), 30-35% of northern taiga wetlands, (mainly southern part) 10-15% of woodlands along the rivers, small areas (< 3%) along the rivers are covered by forests
2	quadrangle with vertices at (66°19'N 71°00'E), (65°55'N 71°42'E), (65°55'N 70°34'E) and (66°19'N 70°23'E)	2500	>50% of woodlands, ca 20% in the north –dry and wet tundra ca 5% in the south – northern taiga
3	quadrangle with vertices at (65°49'N 72°07'E), (65°26'N 72°23'E), (65°15'N 71°32'E) and (65°21'N 71°05'E)	2000	30-40% - northern taiga forests, 30-40% - northern taiga wetlands, 20% – woodlands

Table 2. Classification of vegetation classes based on growing degree-days (GDD_5) and dryness index (DI) (Tchebakova et al., 1994)

Vegetation class	GDD_5 (°C day)	DI
Tundra	0-300	< 3.3
Spruce-larch forest – tundra	300-500	< 2.0
Dark-needled northern taiga	500-800	< 2.3
Dark-needled middle taiga	800-1000	< 2.3

Table 3. Data sets used for fire analysis

Data set	Source	Date	Path/Row	Resolution
Landsat-5	US Geological Survey[1]	1987-1988	159/013, 159/014, 161/013, 161/014	30 m
Landsat-7		2000-2002	159/013, 159/014, 161/013, 161/014	30 m
Landsat-8		2016	159/013, 159/014, 160/013, 160/014, 161/013, 161/014	30 m
Landsat-8		2017-2018	159/013, 159/014, 160/013, 160/014, 161/013, 161/014	30 m

[1] https://earthexplorer.usgs.gov

Table 4. Relations between Landsat mosaic years and the years of major fires

Satellite image year	1968	1988	2001	2016	2018
Preceding major fire year	between 1953[1] and 1964[2]	1976[2]	1990[3]	2012[3]	2016[3]

[1] Chekunova V.S., Geological and geomorfological survey of a part of the lower reaches of the River Nadym basin and parts of the right bank of the River Ob in Nadym region in 1953. VSEGEI: 1954. 72 p.

[2] Corona images, https://earthexplorer.usgs.gov

[3] Landsat images, https://earthexplorer.usgs.gov

Table 5. Data sets used for the analysis of vegetation dynamics

Data set	Source	Date	Path/ map sheet number	Resolution
Corona/KH-4b	US Geological Survey[1]	21.08.1968	DS1104-2217DA(24…45)	≈ 2 m
'Resurs-P' 1,2	Roscosmos[2]	07.11.2016 04.07.2016 28.09.2016	7081_05 8513_02 9830_01	1.6 m
SPOT-6,7	YandexMaps/ AirbusDS[3]	2016-2017	-	1.5 m
Digital elevation model ArcticDEM, v. 3.0	National Geographic Agency, US[4]	2018 (survey 2010-2017)	52_63_2_2, 52_64_1_1, 52_64_1_2, 52_64_2_2, 52_64_2_1, 52_65_1_2, 53_62_2_1, 53_62_2_2, 53_63_2_2, 53_63_1_1, 53_63_1_2, 53_63_2_1, 53_64_2_1, 53_64_1_2, 53_64_1_1, 53_65_1_1, 54_63_2_2, 54_63_2_1, 54_63_1_1, 54_64_1_2, 54_64_1_1	2 m
Topographic maps	Rosreestr[5], Ilyina et al., 1985, Supplementary material	1968-1971	Q-42-57,58; Q-42-59,60; Q-42-69,70; Q-42-71,72; Q-42-81,82; Q-42-83,84; Q-42-95,96; Q42-107,108; Q-43-27,28; Q-43-29,30; Q-43-37,38; Q-43-39,40; Q-43-41,42; Q-43-43,44; Q-43-49,50; Q-43-51,52; Q-43-53,54; Q-43-55,56; Q-43-61,62; Q-43-63,64; Q-43-65,66; Q-43-67,68; Q-43-73,74; Q-43-75,76; Q-43-77,78; Q-43-79,80; Q-43-85,86; Q-43-89,90; Q-43-91,92; Q-43-103,104	1:100 000
NDVI Landsat	US Geological Survey[1]	30.06.2018	160/014-160/013	30 m

[1] https://earthexplorer.usgs.gov
[2] https://gptl.ru
[3] https://yandex.ru/maps
[4] https://arctic-nga.opendata.arcgis.com
[5] https://www.marshruty.ru/Maps/Maps.aspx

Table 6. Change in vegetation class at meteorological stations in accordance with Table 2 (after Tchebakova et al., 1994)

Meteorological station	Vegetation class, 1960s	Vegetation class, 2010s
Nadym	Dark-needled northern taiga	Dark-needled middle taiga
Nyda	Dark-needled northern taiga	Dark-needled northern taiga
Novy Port	Spruce-larch forest-tundra	Dark-needled northern taiga

Table 7. Number of checkpoints (percentage of all checkpoints within a vegetation class, %) corresponding to vegetation shift in fire-affected and non-disturbed dry tundra

State of vegetation	South tundra, fires	Forest-tundra, fires	Northern taiga, fires	South tundra, non-disturbed	Forest-tundra, non-disturbed	Northern taiga, non-disturbed
No shift	5 (71.6)	7 (15.2)	64 (58.7)	107 (93.9)	57 (85.1)	44 (86.3)
To woodlands	1 (14.3)	13 (28.3)	30 (27.5)	7 (6.1)	10 (14.9)	7 (13.7)
To forests	1 (14.3)	26 (56.5)	15 (13.8)	0 (0)	0 (0)	0 (0)
All	7 (100)	46 (100)	109 (100)	114 (100)	67 (100)	51 (100)

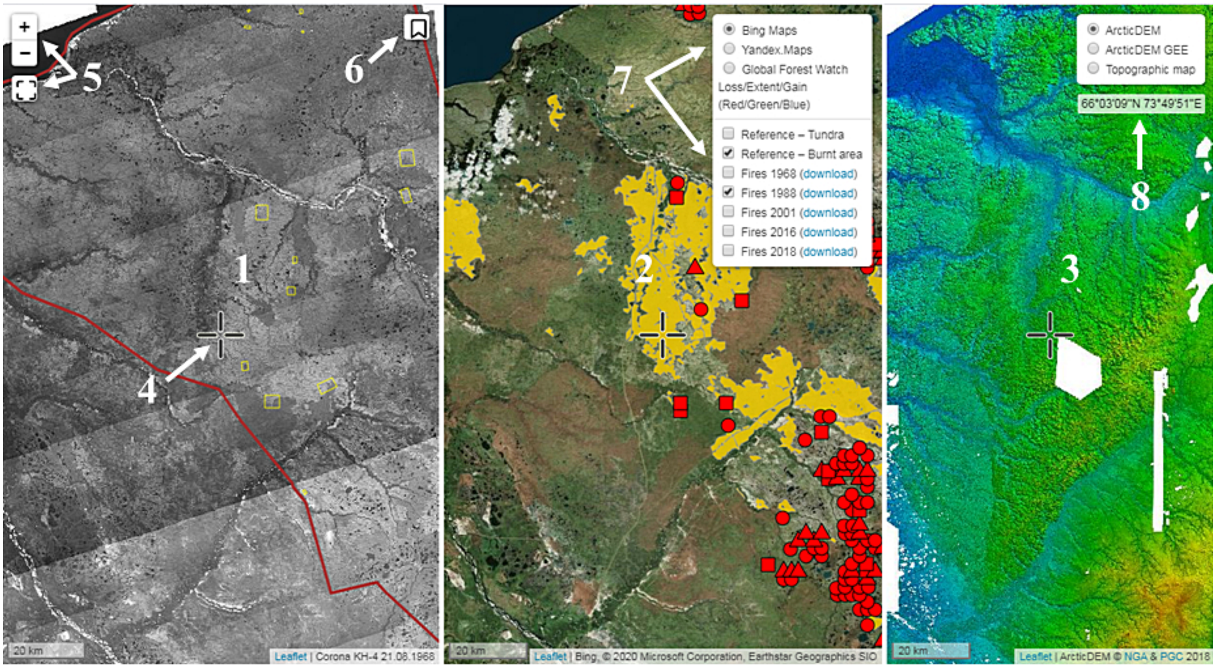

Figure A1. Interface of geoportal NC 50: 1 – map 1; 2 – map 2; 3 – map 3; 4 – map pointer; 5 – zoom; 6 – widget containing bookmarks of the reference sites; 7 – panel of base maps and layers; 8 – current coordinates.

Figure B1. Illustration of vegetation cover in the photos from the field campaign: the non-disturbed site (left panel) and the nearby site affected by fires before 1968 and 1988 (right panel).

Table B1. Field observations of vegetation and active layer thickness

Site	Active layer thickness (cm)	Vegetation cover, dominant species
65°50’59.49"N, 74°23’03.91"E – non-disturbed	38.3 (min 38, max 40, n=3)	lichen (*Cladonia alpestris*, *Cladonia rangiferina*, *Cetraria nivalis*) – up to 40%, shrubs (*Betula nana, Ledum palustre*) – up to 70%, cloudberry (*Rubus chamaemorus*) – up to 5%
65°50’51.14"N 74°24’58.39"E – fire before 1968 and 1988	119.0 (min 90, max 170, n=10)	lichen (*Cladonia alpestris, Cladonia rangiferina, Cetraria nivalis*) – up to 60%, shrubs (*Betula nana, Ledum palustre, Vaccínium uliginósum*) – up to 80%, mosses (*Polytrichum commune*) – up to 50%
65°56’18.27"N 74°38’59.00"E – fire before 1988	102.0 (min 70, max 130, n=5)	lichen (*Cladonia alpestris, Cladonia rangiferina, Cetraria nivalis*) – up to 20%, shrubs (*Betula nana, Ledum palustre, Vaccínium uliginósum*) – up to 70%, mosses (*Polytrichum commune*) – up to 30%